


Kinetically constrained model for gravity-driven granular flow and cloggingGregory Bolshak,^{1,*} Rakesh Chatterjee,¹ Rotem Lieberman,² and Yair Shokef^{1,†}¹*School of Mechanical Engineering and Sackler Center for Computational Molecular and Materials Science, Tel Aviv University, Tel Aviv 69978, Israel*²*Rafael Advanced Defense Systems, Haifa 31021, Israel* (Received 4 June 2019; revised manuscript received 5 September 2019; published 24 September 2019)

We add extreme driving to the Kob-Andersen kinetically constrained lattice-gas model in order to mimic the effect of gravity on dense granular systems. For low particle densities, the current that develops in the system agrees at arbitrary field intensity with a mean-field theory. At intermediate densities, spatial correlations give rise to nonmonotonic dependence of the current on field intensity. At higher densities, the current ultimately vanishes at a finite, field-dependent density. We supplement the study of this bulk behavior with an investigation of the current through a narrow hole. There, lateral flow decreases the local density in front of the hole. Remarkably, the current through the hole quantitatively agrees with a theoretical prediction based on the bulk current at the measured local density.

DOI: [10.1103/PhysRevE.100.032137](https://doi.org/10.1103/PhysRevE.100.032137)**I. INTRODUCTION**

Jamming is the transition from a flowing state to a rigid or arrested state as density increases in an assembly of particles [1,2]. Colloidal suspensions, glass-forming liquids, and granular materials show heterogeneous dynamics as they approach jamming [3–10]. Clogging is when the flow of granular materials through a bottleneck [11–14] or pipe [15] ceases to exist. Jamming is a bulk phenomenon that occurs throughout the system, while clogging is identified as the inability to flow through a specific narrow region in the system where particles get stuck locally. This eventually causes the flow to stop also in other regions. There have been studies of the crossover between jamming and clogging in heterogeneous environments [16]. Many systems in nature and in industrial applications exhibit jamming or clogging in very complicated geometries [17,18], and it is important to understand how confinement induces the jamming or clogging of granular matter. Experiments on granular systems [19] show steady growth in dynamical heterogeneity as the relaxation time increases with increasing density. We employ kinetically constrained models [20–25] to construct a lattice model for describing the physical mechanisms involved in jamming. These models do not rely on any type of interaction between the particles other than excluded volume interaction and are supplemented by specific kinetic rules that control the movement of particles depending on the local density around them. These dynamical restrictions yield glassy behavior in the system. Specifically, as the density of particles on the lattice increases, relaxation dynamics become dramatically slow and heterogeneous. In certain situations this slowing down can even lead to complete jamming, in which particles will never flow [26–32].

In this paper, we examine the effect of an external field on jamming in the two-dimensional Kob-Andersen [33] lattice

gas with kinetically constrained dynamical rules. We implement the external field in a way that, to our understanding, better represents gravity-driven flow of granular materials, compared to previous studies [20,21,34–36]. We measure the bulk current as a function of density and observe that the current vanishes at a jamming density which depends on the applied external field. We also measure the bulk current as a function of the external field and find an unexplained nonmonotonicity as a function of field. To understand the microscopic origin for the dynamically jammed states, we find that these states exhibit some rare mobility regions along with other regions of higher mobility due to local relaxation. Increasing or decreasing local mobility in some region sometimes facilitates the overall cooperative dynamics of the system. Furthermore, we study the effect of confinement on clogging by investigating the behavior of the system when particles are allowed to pass through a narrow orifice. We quantitatively explain the measured current in terms of the current of an effective bulk system with the local density that we measure in front of the orifice.

The paper is structured as follows. In Sec. II, we introduce our model and describe the numerical simulation details. In Sec. III, we study the bulk current as a function of external field and show the nonmonotonic behavior of the current. We measure two-point density correlations, focus on the microscopic structure of the system at different parameter regimes, and obtain the jamming phase diagram vs density and field. In Sec. IV, we study our model with confinement, which mimics the flow of particles through an orifice. Section V summarizes the work.

II. MODEL

We use the Kob-Andersen kinetically constrained model [33], in which particles are randomly distributed on the square lattice with density ρ and they randomly attempt to move in one of four possible directions. According to this model, the move is allowed only if the target site is vacant and if there

*gregory7@mail.tau.ac.il

†shokef@tau.ac.il

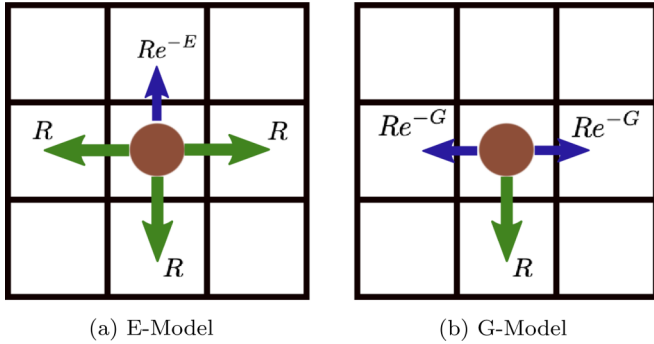


FIG. 1. (a) E model: Each particle has a fixed rate to move in three direction denoted by green arrows, and a reduced rate to move against the direction of the field, as shown by the shorter blue arrow. (b) G model: Each particle has a fixed rate to move in the direction of the field, as shown by the green arrow, and a reduced rate to move in each of the transverse directions, as shown by the shorter blue arrows, with no movement against the direction of the field. In both models, moves succeed only if the Kob-Andersen kinetic constraints are satisfied.

are at least two vacant nearest neighbors before and after the move. An external field may be applied in some preferred direction in a manner which we will refer to as the *E model* [20,21]. Then, each particle has a rate R to move along the field or in each of the transverse directions, whereas there is a reduced rate Re^{-E} for particles to move against the external field; see Fig. 1(a).

We suggest that in gravity-driven granular flow, particles move mainly along the direction of the gravitational field, they have negligible ability to move against the field, and due to collisions with other particles they have some limited ability to move in the transverse directions. The rate of motion along the field should be substantially higher than in the transverse directions. Thus we introduce the *G model* with a constant rate R to move along the field, together with transverse movement with a reduced rate Re^{-G} , and no movement against the field, as shown in Fig. 1(b). Here particles have a constant rate to attempt moving in the direction of the field G , and particle current changes by varying the lateral motion, which in turn influences the acceptance rate of moves along the field. Note that the extreme driving limit of the E model, $E = \infty$, is equivalent to $G = 0$ in the G model. Thus by increasing G , we are changing the rate of motion in the transverse direction and thus extending the E model to even more extreme driving.

Note that the E model allows moves also against the field and thus satisfies detailed balance, similarly to the asymmetric simple exclusion process (ASEP) model. In these models, for any allowed move also the reverse move is allowed at some finite rate. This implies that in the E model the initial configuration sets whether the system will eventually jam or not [10]. The G model on the other hand has finite rate for some of the motions along the field and zero rate for the time-reversed moves, against the field. Thus it violates detailed balance, similarly to the totally asymmetric simple exclusion process (TASEP) model [37], and in the G model jamming or clogging is a result of the system being dynamically attracted to some static absorbing state.

III. BULK CURRENT

In order to understand the behavior of the G model precisely, we study the dynamics of the system in various regimes. Here we begin with the bulk behavior and consider a large system with periodic boundary condition in both directions. In the low-density regime, we expect correlations to be weak and therefore we can predict the current of the particles in the direction of the field. We define the occupancy index $\eta_{i,j}$ for each site (i, j) in the two-dimensional lattice as

$$\eta_{i,j} = \begin{cases} 1, & \text{the site is occupied,} \\ 0, & \text{the site is vacant.} \end{cases}$$

Now we can write the mean current in the direction of the field, based on the kinetic constraints. It can be clearly seen from Fig. 2 that when a particle at $(0,0)$ attempts to move to the vacant site $(0,1)$, then at least one of the three neighboring sites denoted by blue must be empty along with at least one of the three sites denoted by light green that must also be empty to satisfy the kinetic constraint. Therefore the current reads

$$J = \langle \eta_{0,0}(1 - \eta_{0,1})(1 - \eta_{-1,0}\eta_{0,-1}\eta_{1,0})(1 - \eta_{-1,1}\eta_{0,2}\eta_{1,1}) \rangle. \quad (1)$$

Assuming no correlations between the occupancy of neighboring sites, we obtain the mean-field (MF) current,

$$J_{MF}(\rho) = \rho(1 - \rho)(1 - \rho^3)^2. \quad (2)$$

We run kinetic Monte Carlo simulations with a Bortz-Kalos-Lebowitz rejection-free algorithm [38], which makes the simulations very efficient, on a periodic lattice of dimension $L \times L$ and typically use $L = 400$. We verified convergence by comparing to simulations with $L = 800$. We typically average over 100 realizations starting from different random initial conditions. We first allow the system to relax for $t = 10^6$ time units and then start measuring the current after the system has reached the steady state. We compare our numerical result with the MF current, first in the two extreme limits: $G = 0$ and $G = \infty$, having only longitudinal motion in the latter case.

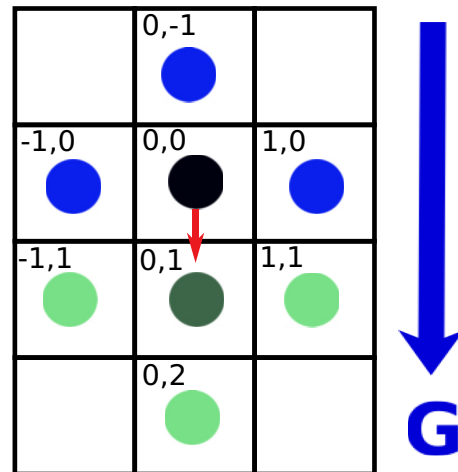


FIG. 2. When a particle at position $(0,0)$ attempts to move one step in the direction of the field, the target site $(0,1)$ should be vacant, but also at least one of the (blue) sites neighboring the origin site and at least one of the (light green) sites neighboring the target site should be vacant to obey the kinetic constraint.

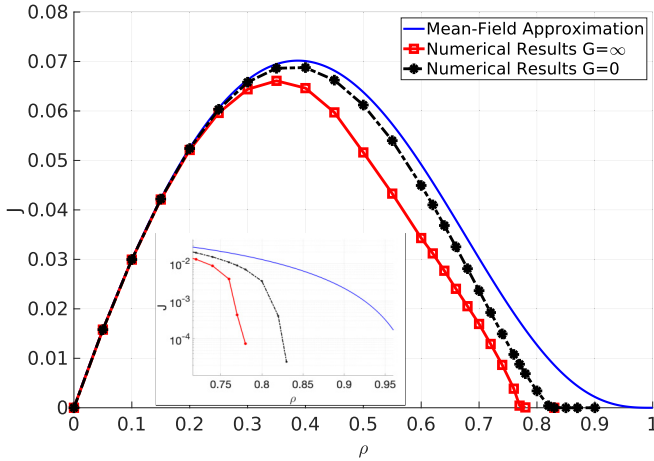


FIG. 3. Current as a function of density in simulations in two regimes: $G = 0$ (black) and $G = \infty$ (red) along with MF approximation from Eq. (2) (blue). They agree at low densities, above which deviations from MF and dependence on G start to appear due to increasing correlations. Zoomed plot in the inset shows the density range where current vanishes.

Figure 3 shows good agreement with the MF approximation, given in Eq. (2), in the low-density regime. As follows from this MF approximation, there is no dependence on the field G at all. Above $\rho \approx 0.2$, correlations start playing a substantial role and the observed current is lower than the MF prediction. As G increases, the rate to move in the direction transverse to the field is lower, thus creating more constrained dynamics, leading to stronger deviation from MF behavior. We also observe that although our MF theory predicts $J > 0$ for any density $\rho < 1$, in our simulations the current stops at some finite density, which is dependent on the field G . Specifically, for $G = 0$, jamming occurs at $\rho = 0.83$ and for $G = \infty$, it occurs at $\rho = 0.78$. This jamming at finite density has been observed in the $E = \infty$ limit of the E model [20], which coincides with our $G = 0$ limit.

Note that these values of the jamming density are significantly lower than what we would expect in the Kob-Andersen model at such system sizes without driving. Although in the thermodynamic limit the undriven model jams only at $\rho = 1$ [26], finite-size effects lead to jamming at $\rho_c = 1 - \frac{\lambda}{\log L}$, where λ may be approximated by $\lambda = 0.25$ [27]. Thus for our $L = 400$ system size, this would lead to $\rho_c = 0.96$, which is much higher than the densities at which we observe jamming in our driven model. Thus we suggest that the phenomenon we observe here is not a finite-size effect.

To further understand this jamming at finite density, we consider narrow channels. Namely we simulate rectangular systems of dimension $L_x \times L_y$, where the system size L_y in the driving direction is verified to be large enough, and the system size L_x in the lateral direction takes small values. We employ periodic boundary conditions in both directions and concentrate here on the extreme driving limit $G = \infty$. Figure 4 shows how even extremely narrow channels ($L_x = 2, 3$) exhibit the same qualitative behavior as the bulk results. Note that for narrow systems, at any density there is a finite probability to have at least two consecutive fully occupied

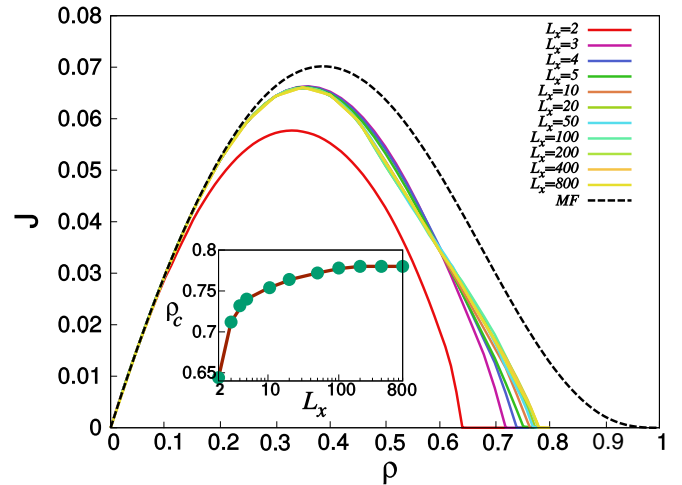


FIG. 4. Current as a function of density for systems of various width L_x , as indicated in the legend. Dashed line is the MF result (2). All simulations are with $L_y = 800$. Inset shows critical density for jamming vs channel width.

rows within the system [28]. Due to the kinetic constraint, these particles will never be able to move. Thus the current vanishes for such initial conditions, and we exclude them from the averaging over all random initial conditions. It would be interesting to consider this simple limit, in which analytical progress may be obtained. Moreover, this geometry could link between clogging and jamming, as we discuss in detail when considering confined geometries below.

A. Current as a function of G

We simulated the steady state current behavior as a function of the external field G . The results of the simulation for varying G values can be seen in Fig. 5. For each density, we normalize the current by the MF prediction according to Eq. (2). As we have already seen, the substantial deviation

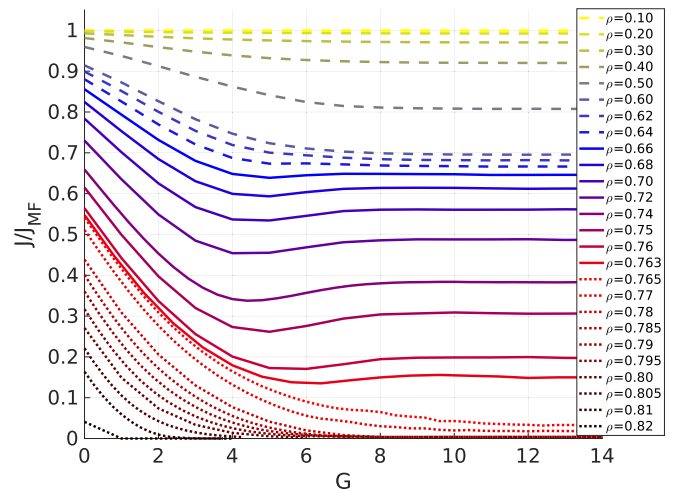


FIG. 5. Normalized current J/J_{MF} as a function of the external field G . For lower densities, the deviation from the mean-field current is small. This deviation increases as we increase G . As the density grows, the current becomes nonmonotonic as a function of G for $0.66 \lesssim \rho \lesssim 0.76$ (solid lines).

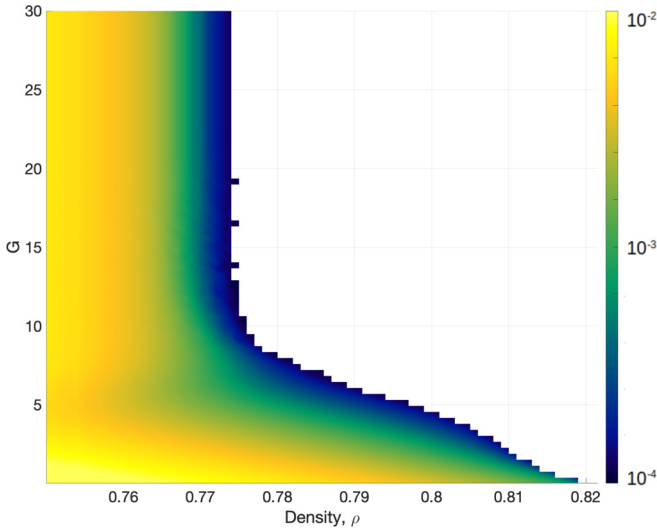


FIG. 6. Phase diagram in the density-field plane showing the jamming transition. The colored region is the flowing state with steady state current values depicted in the color bar, and the white space is the jammed state, in which the current vanishes.

from the MF result, and the significant dependence on G , both take place at higher densities. This can be understood by the fact that the rate to move sideways controls the probability to get stuck in the way. Whenever the rate to move sideways is large (G is low), there is a higher probability that a particle will change its trajectory and hence will be less correlated, causing the current to increase at lower values of G .

Remarkably, in a finite region of densities, $0.66 \lesssim \rho \lesssim 0.76$, the dependence on G becomes nonmonotonic and there is a region where the current slightly increases as we increase G before the current approaches its asymptotic value at higher values of G . At this point we do not have a theoretical explanation for how correlations that develop in the system cause the deviation from MF behavior to be nonmonotonic as a function of the external field.

B. Jamming phase diagram

According to our MF prediction, the current asymptotically vanishes only as the density approaches unity. However, from the numerical observations, one can see that there is some field-dependent critical density $\rho_c(G)$ at which the particles are arrested and the system gets jammed. Specifically, Fig. 3 shows that the current goes to zero at different densities for $G = 0$ and $G = \infty$. This implies that such jamming effect depends on the field intensity G . In order to investigate the transition from free flow to a jammed state, we show in Fig. 6 the phase diagram, which describes the numerical results of the current as a function of the density and field. The transition to the jammed state happens in the density range $0.78 < \rho_c(G) < 0.83$, where as density increases, a smaller field is required to get the jammed phase.

C. Correlation analysis

We have performed correlation analysis by defining the two-point density correlation function as

$$C_2(\Delta x, \Delta y) = \frac{\langle \eta_{i,j} \eta_{i+\Delta x, j+\Delta y} \rangle - \rho^2}{\rho - \rho^2}. \tag{3}$$

The normalization in the denominator comes from the fact that at $\Delta x = \Delta y = 0$, we get $\langle \eta^2 \rangle = \rho$ because the occupancy index satisfies $\eta^2 \equiv \eta$, and the density ρ is the dimensionless fraction of occupied sites out of the total number of sites in the lattice. As can be seen from Fig. 7, the correlations are mostly longitudinal as G becomes stronger. This is because increasing G is equivalent to decreasing the probability to move in the transverse direction, which corresponds to the dominant motion being longitudinal.

D. Analysis of microscopic structure

One of the prominent differences between various regimes of G values are the internal structures that are formed in the steady state. As the density increases, the homogeneously distributed particles start to create clusters of particles and clusters of holes, as can be seen in Fig. 8. At high densities, the

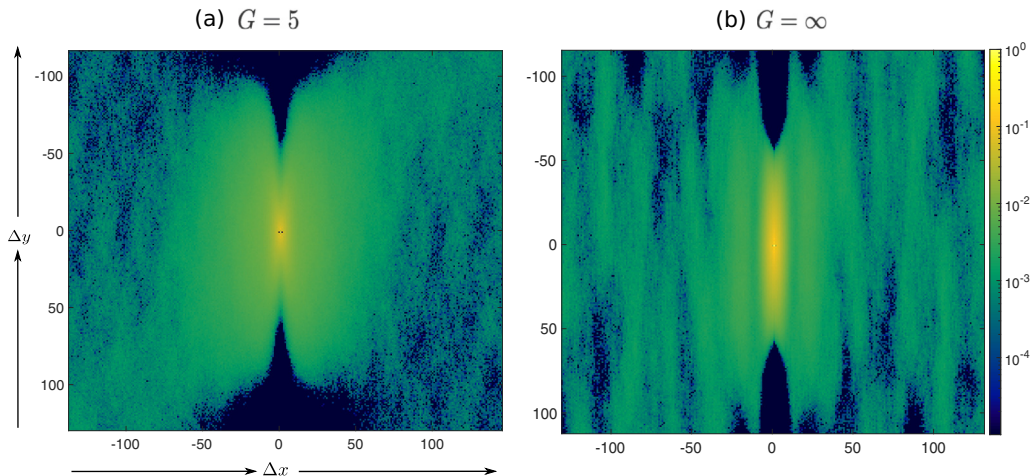


FIG. 7. Two-point density correlation function in the steady state with a system size $L = 400$ having density $\rho = 0.7$. Left and right panels are for $G = 5$ and $G = \infty$, respectively.

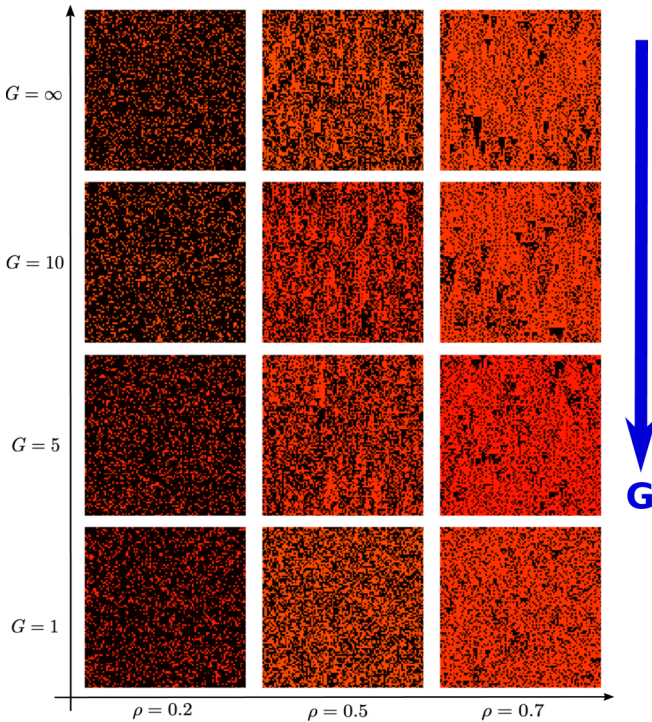


FIG. 8. Structures of particles (red) and holes (black) in steady state for different values of field and density.

typical shapes of the microscopic structures of vacancies are illustrated in Fig. 9(b). These start with the formation of rows of holes perpendicular to the applied field, and are referred to as shear bands [21]. These shear bands basically act as barriers to the flow, below which there are areas of vacancies, which go around these barriers and, due to transverse motion, gradually fill in these areas of vacancies.

As can be seen from Fig. 9(a), for small values of G , the height of the vacancy region is typically small, as there is a high transverse motion, and the particles fill the open space below the shear bands relatively quickly, as opposed to the typical structure of the hole cluster for high values of

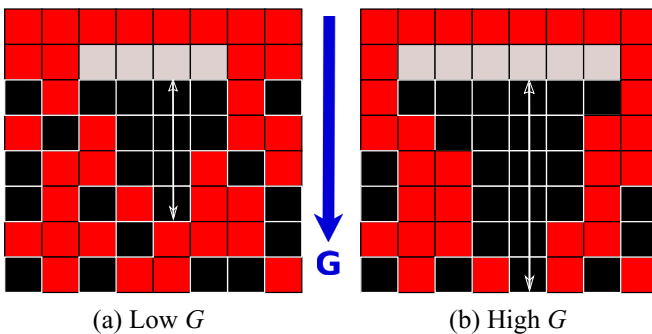


FIG. 9. (a) Typical structure of the hole clusters for small values of G . The smaller shear band (bright gray), together with a higher moving rate in the transverse direction, results in a smaller height of the hole cluster. (b) Typical structure of the hole clusters for high values of G . Lower transverse rate results in a higher height to fill in the vacancies below the wider shear band. Red indicates occupied sites. Black denotes vacant sites.

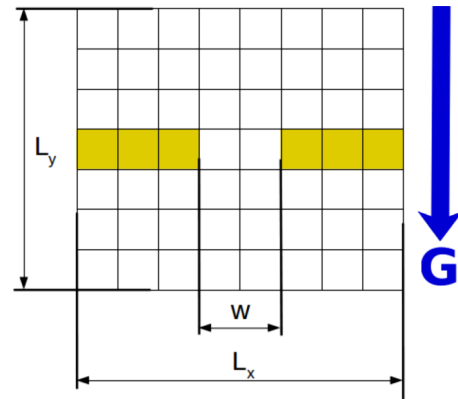


FIG. 10. Schematic diagram of a narrow opening of width w within a horizontal wall of immobile particles (yellow).

G , as illustrated in Fig. 9(b). As we further observe, these hole clusters are not persistent and they dynamically form and get destructed in the steady state. The evolution of the configuration at the steady state and the appearance of the hole clusters can be seen in Fig. 8. This effect starts taking place at high densities. For $G = \infty$, there is no motion at all in the transverse direction and the only motion is in the direction of the field. In this case, it can be seen that the hole clusters are the longest, as depicted in Fig. 9(b).

IV. FLOW THROUGH AN ORIFICE

In this section, we study our model with confinement that mimics the behavior of discharging granular materials through an opening [39]. The confinement reveals new phenomena, such as density heterogeneity and clogging of the system near the opening. In addition, we would like to investigate the confined flow and to reveal its connection to the jamming of the bulk current, discussed in Sec. III.

We define a confined geometry imitating the discharge of grains through an orifice, as shown in Fig. 10. Also in this geometry, we employ periodic boundary conditions in both directions. At the center of the lattice we place a rigid horizontal barrier, with a narrow opening of width w . This obstacle is achieved by artificially placing one row of occupied sites in the initial condition and not moving them during the simulation. Due to the periodic boundary conditions, this geometry is equivalent to infinitely many openings with distances $L_x - w$ in the transverse direction, and infinitely many such barriers at a distance L_y in the longitudinal direction. In order to eliminate finite size effects, we verified that the ratio L_x/w is large enough. We show results from simulations with $L_x = 180$, but found very small changes when increasing system width to $L_x = 600$.

The simulation begins with randomly and uniformly distributed particles throughout the lattice. Due to the presence of the barrier, there is sedimentation of the particles toward the barrier. This sedimentation depends on the initial density and on the strength G of the field. It would be interesting to relate this to experiments with colloidal suspensions [40]. In front of the opening there is flow. As a result, heterogeneity of the density develops. For $G < \infty$, due to lateral motion, particles rearrange, such that the density above the barrier

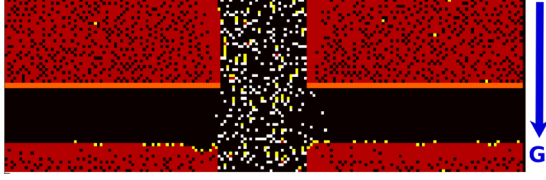


FIG. 11. Snapshot of particle configuration in a lattice of dimension 60×180 with an orifice of width $w = 30$, at field $G = 1$, and density $\rho = 0.5$. The system is in steady state that was reached after 10^6 units of time. Red (dark) particles are stuck (nonmovable in any direction), white particle can move in the direction of the field, yellow (bright) particles can move only sideways, and black sites are empty.

increases, and by mass conservation, the density above the opening decreases, as shown in Fig. 11. We also observe that in the steady state, the only contributing part to the current is the flow above the orifice, denoted by the white particles in Fig. 11. This is because the system is jammed in other regions of the lattice, as shown by the red particles.

We are interested in measuring the *total current* of particles through the opening, namely the number of particles flowing through the opening per unit time as given by

$$J_{\text{tot}} = \frac{\langle N \rangle}{tL_y}, \quad (4)$$

where $\langle N \rangle$ is the average number of particles that moved along the direction of the field during the time interval t anywhere in the lattice, and L_y is the lattice height (see Fig. 10). Using this definition, we can now estimate the total current through the orifice using the bulk current, which we studied in Sec. III. Recalling that the bulk current is defined as the number of particles flowing in the system per unit time and per lattice size, we can formally define the bulk current as $J_{\text{bulk}} = \langle N \rangle / (tL_xL_y)$. In order to be consistent with the definition of the total current in Eq. (4), our crudest approximation will be as follows,

$$J_{\text{tot}} = J_{\text{bulk}}(\rho, G)w. \quad (5)$$

Figure 12 shows results of numerical simulation, in which we calculated the total current through the orifice, in comparison to the crude approximation given in Eq. (5). As we can see from the plot, there is a considerable discrepancy between the numerical results (blue points) and this calculation (black line). To explain this, we recall that the density in the confined system is heterogeneous, and in particular, the density ρ_{local} above the orifice is lower than the average density ρ in the system. Hence we consider the local density measured above the orifice, as this is the only region that contributes to the current in the steady state. This corrects our theoretical prediction to

$$J_{\text{tot}} = J_{\text{bulk}}(\rho_{\text{local}}, G)w. \quad (6)$$

In Sec. III, we have seen that at the low-density regime in nonconfined systems, the bulk current is higher for lower densities. Remarkably, the analytical expression (6) that takes into account the reduced local density above the opening for the total current coincides with the numerical results, as seen

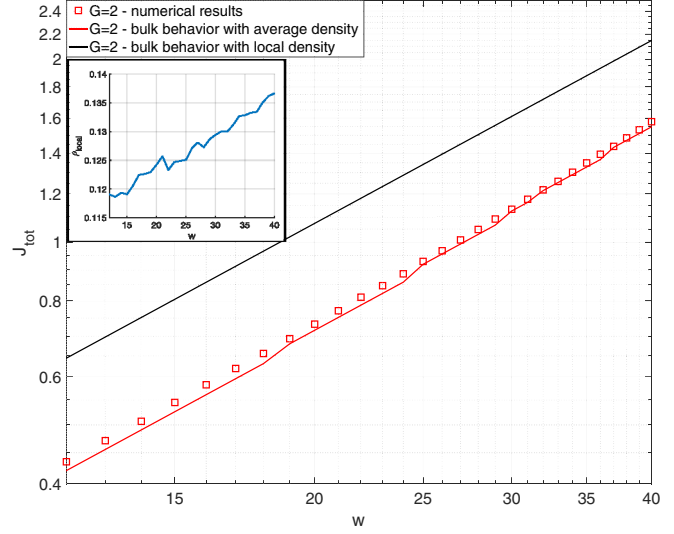


FIG. 12. Total current J_{tot} vs orifice width w at bulk density $\rho = 0.5$ with $G = 2$ in a (60×180) lattice. Analytical expression Eq. (5) using bulk density (black) does not match with simulation (red squares), whereas the analytical expression Eq. (6) using local density (red) shows a very good agreement with simulation. Inset: Local density above the opening vs opening width.

in Fig. 12. Thus, using the behavior studied for the bulk system, we can predict the dynamics in confined systems. We perform a similar comparison also for different values of G . As the field increases, the transverse motion becomes less probable due to a lower rate to move in that direction. This leads to a longer time needed to reach the steady state in confined systems. In Fig. 13 we show the numerical results for two different values of G with remarkable agreement with the same analytical prediction, described by Eq. (6). As w becomes smaller, the current decreases linearly with

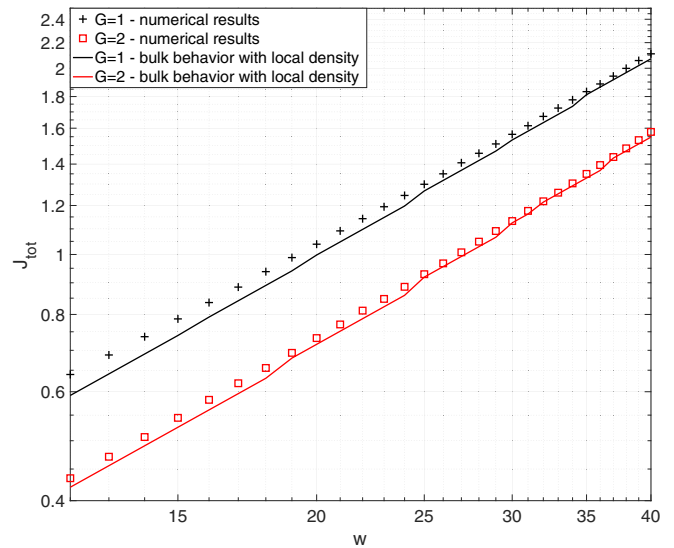


FIG. 13. Total current J_{tot} vs orifice width w for $G = 1$ (black) and $G = 2$ (red) at bulk density $\rho = 0.5$. Data points from numerical simulation and solid lines from analytical expression Eq. (6) using the local density measured in the simulations.

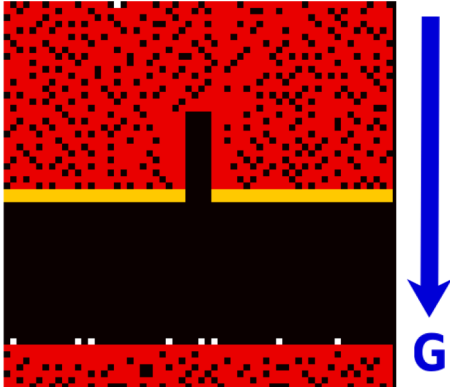


FIG. 14. Clogged configuration achieved with bulk density $\rho = 0.5$, opening width $w = 4$, and field $G = 1$. Lattice size 60×60 .

w , as Eq. (6) predicts. Note that our analytical estimation of the current (6) seems to be systematically lower than the numerical observation. It would be interesting to understand the reason for this difference.

For very small values of w , we obtain clogging of the particles near the opening and the overall current ceases for some realizations. The numerical results shown in Figs. 12 and 13 are obtained by averaging over the current from many realizations that were not clogged. This clogging state becomes more and more probable as w becomes smaller, and it would be interesting to study it further. When clogging appears near the opening, the particles form a rectangular structure, as can be seen in Fig. 14. This particular structure is the result of the kinetic constraints, for which neither of the surrounding particles near the opening can move.

V. CONCLUSIONS

We studied the behavior of granular materials subjected to a gravitational field in a confined geometry. To that end, we used the kinetically constrained Kob-Andersen model, which implements simple dynamics of a lattice gas, with no interactions between neighboring particles, but with kinetic rules that depend on the occupancy of neighboring sites. Such a description allows us to employ efficient numerical simulations. In order to simulate the gravitational field, we modified the rates of the moves in the direction perpendicular to the field, controlled by the parameter G , and did not allow moves against the direction of the field. We first studied the bulk behavior of the model, eliminating confinement by creating a large system with periodic boundary conditions. We built a MF theory and performed numerical simulations

in order to understand the range of validity of the MF theory and the role of correlations. For that purpose, we constructed an efficient rejection-free algorithm, in which we skip all the unsuccessful moves. We observed that at the range of densities $0.66 \lesssim \rho \lesssim 0.76$ the current exhibits nonmonotonic behavior as a function of the driving field G . From the microscopic point of view we see that at the high-density regime, close to jamming, the spatial distribution of the particles is very heterogeneous; namely, there are spatial structures of holes that are dynamically formed and destructed as a result of the development of shear bands.

To study discharge through a narrow opening, we defined a confined geometry in our 2D lattice by introducing a horizontal barrier with an opening of some size that we could change. We conducted numerical simulations, measuring the total current through the opening, and revealed two phenomena: clogging close to the opening and highly reduced density of the flowing particles. We measured the spatial distribution of the particles in the steady state with confinement, measuring only the current above the opening, as this is the only contributing part to the current in the whole system. We were able to analytically predict the current as a function of the opening width by using the bulk current corresponding to the reduced local density, as measured from numerical simulations with confinement. We obtained excellent agreement between the total current through the opening from numerical simulation and the analytical calculation based on the current measured in the bulk case, corresponding to the reduced local density above the opening.

One of our most remarkable observations for bulk behavior is the nonmonotonicity of the current as a function of field intensity at intermediate densities. Further structural analysis could identify the reason for this behavior.

Similar studies of discharge through an opening and related phenomena such as spatial density heterogeneity and bottleneck clogging have already been seen in granular matter, whether in experiments or simulations. Our model reveals qualitatively the same phenomena, whereas thanks to its simplicity the simulations are fast and can be done on very large systems. The model can also be extended to three dimensions where, instead of looking on the square lattice, one may consider the cubic lattice. This case may perhaps be more suitable for comparison with actual granular experiments.

ACKNOWLEDGMENTS

We thank David Gomez, Erdal Oguz, Daniel Vilyatser, Eyal Rubin, Nimrod Segall, Hadas Shem-Tov, and Eial Teomy for helpful discussions. This research was supported by Israel Science Foundation Grant No. 968/16 and by the Prof. A. Pazy Research Foundation.

- [1] A. J. Liu and S. R. Nagel, *Nature (London)* **396**, 21 (1998).
- [2] M. van Hecke, *J. Phys.: Condens. Matter* **22**, 033101 (2010).
- [3] L. Berthier and J. P. Garrahan, *Phys. Rev. E* **68**, 041201 (2003).
- [4] S. Léonard and P. Harrowell, *J. Chem. Phys.* **133**, 244502 (2010).

- [5] R. Pastore, M. Pica Ciamarra, and A. Coniglio, *Fractals* **21**, 1350021 (2013).
- [6] J. P. Garrahan and D. Chandler, *Phys. Rev. Lett.* **89**, 035704 (2002).
- [7] L. Berthier and J. Garrahan, *J. Chem. Phys.* **119**, 4367 (2003).

- [8] E. Marinari and E. Pitard, *Europhys. Lett.* **69**, 235 (2005).
- [9] S. Whitelam, L. Berthier, and J. P. Garrahan, *Phys. Rev. E* **71**, 026128 (2005).
- [10] E. Teomy and Y. Shokef, *Phys. Rev. E* **92**, 032133 (2015).
- [11] K. To, P. Y. Lai, and H. K. Pak, *Phys. Rev. Lett.* **86**, 71 (2001).
- [12] I. Zuriguel, A. Garcimartín, D. Maza, L. A. Pugnaloni, and J. M. Pastor, *Phys. Rev. E* **71**, 051303 (2005).
- [13] I. Zuriguel, A. Janda, A. Garcimartín, C. Lozano, R. Arévalo, and D. Maza, *Phys. Rev. Lett.* **107**, 278001 (2011).
- [14] C. Lozano, A. Janda, A. Garcimartín, D. Maza, and I. Zuriguel, *Phys. Rev. E* **86**, 031306 (2012).
- [15] F. Verbücheln, E. Parteli, and T. Pöschel, *Soft Matter* **11**, 4295 (2015).
- [16] H. Péter, A. Libál, C. Reichhardt, and C. J. O. Reichhardt, *Sci. Rep.* **8**, 10252 (2018).
- [17] See <http://www.rocksystems.com/machinery/conveyors>.
- [18] R. A. Bagnold, Geological Survey Professional Paper No. 422-I, 1966, <http://pubs.usgs.gov/pp/0422i/report.pdf>.
- [19] A. R. Abate and D. J. Durian, *Phys. Rev. E* **76**, 021306 (2007).
- [20] M. Sellitto, *Phys. Rev. Lett.* **101**, 048301 (2008).
- [21] F. Turci, E. Pitard, and M. Sellitto, *Phys. Rev. E* **86**, 031112 (2012).
- [22] E. Teomy and Y. Shokef, *Phys. Rev. E* **95**, 022124 (2017).
- [23] C. Arita, P. L. Krapivsky, and K. Mallick, *J. Phys. A: Math. Theor.* **51**, 125002 (2018).
- [24] M. Sellitto and J. J. Arenzon, *Phys. Rev. E* **62**, 7793 (2000).
- [25] Y. Levin, J. Arenzon, and M. Sellitto, *Europhys. Lett.* **55**, 767 (2001).
- [26] C. Toninelli, G. Biroli, and D. S. Fisher, *Phys. Rev. Lett.* **92**, 185504 (2004).
- [27] E. Teomy and Y. Shokef, *J. Chem. Phys.* **141**, 064110 (2014).
- [28] E. Teomy and Y. Shokef, *Phys. Rev. E* **86**, 051133 (2012).
- [29] E. Teomy and Y. Shokef, *Phys. Rev. E* **89**, 032204 (2014).
- [30] G. Biroli and C. Toninelli, *Eur. Phys. J. B* **64**, 567 (2008).
- [31] A. Ghosh, E. Teomy, and Y. Shokef, *Europhys. Lett.* **106**, 16003 (2014).
- [32] N. Segall, E. Teomy, and Y. Shokef, *J. Stat. Mech.: Theory Exp.* (2016) 054051.
- [33] W. Kob and H. C. Andersen, *Phys. Rev. E* **48**, 4364 (1993).
- [34] J. Arenzon and Y. Levin, *Phys. A (Amsterdam)* **325**, 371 (2003).
- [35] H. C. Marques Fernandes, J. Arenzon, Y. Levin, and M. Sellitto, *Phys. A (Amsterdam)* **327**, 94 (2003).
- [36] Y. Shokef and A. J. Liu, *Europhys. Lett.* **90**, 26005 (2010).
- [37] B. Derrida, *J. Stat. Mech.: Theory Exp.* (2007) P07023.
- [38] A. B. Bortz, M. H. Kalos, and J. L. Lebowitz, *J. Comput. Phys.* **17**, 10 (1975).
- [39] W. A. Beverloo, H. A. Leniger, and J. van de Velde, *Chem. Eng. Sci.* **15**, 260 (1961).
- [40] S. R. Liber, S. Borohovich, A. V. Butenko, A. B. Schofield, and E. Sloutskin, *Proc. Natl. Acad. Sci. USA* **110**, 5769 (2013).